

SHORT COMMUNICATION

Changes in apparent diffusion coefficients in the normal uterus during different phases of the menstrual cycle

¹A KIDO, MD, PhD, ^{1,2}M KATAOKA, MD, PhD, ¹T KOYAMA, MD, PhD, ¹A YAMAMOTO, MD, PhD, ³T SAGA, MD, PhD and ¹K TOGASHI, MD, PhD

¹Department of Diagnostic Imaging and Nuclear Medicine, Kyoto University, 54 Shogoin Kawaharacho, Sakyo-ku, Kyoto City, Kyoto 606-8507, Japan, ²Department of Radiology, University of Cambridge, Addenbrooke's Hospital, Box 218, Hills Road, Cambridge CB2 0QQ, UK, and ³Molecular Imaging Center, National Institute of Radiological Sciences, 4-9-1 Anagawa, Inage-ku, Chiba 2638555, Japan

ABSTRACT. This study investigated the apparent diffusion coefficients (ADCs) of the uterine zonal structures (myometrium, endometrium and junctional zone) among reproductive women, and their changes during the menstrual cycle. Magnetic resonance (MR) images of seven healthy females (aged 24–31 years) were obtained during the periovulatory, luteal and menstrual phases. Diffusion-weighted imaging (DWI) was performed with a single-shot echo-planar imaging (EPI) sequence in the midsagittal plane of the uterus using three *b*-values (*b*=0, 500 or 1000 s mm⁻²). The ADC values of the three uterine zonal structures were measured on an ADC map by placing two regions of interest (ROI) on the corresponding zonal structures. The average changes of ADC values (intra-individual ADC value variation) over three menstrual phases were $0.41 \times 10^{-3} \text{ mm}^2 \text{ s}^{-1}$ (range, 0.08–0.91) for myometrium, $0.55 \times 10^{-3} \text{ mm}^2 \text{ s}^{-1}$ (0.35–0.84) for endometrium, and $0.40 \times 10^{-3} \text{ mm}^2 \text{ s}^{-1}$ (0.18–0.59) for the junctional zone. The ADC values for myometrium and endometrium were lower in the menstrual phase, although there was some overlap of individual values. Interindividual variation in ADC value for a given zone or phase ranged from $0.48 \times 10^{-3} \text{ mm}^2 \text{ s}^{-1}$ to $0.85 \times 10^{-3} \text{ mm}^2 \text{ s}^{-1}$. Intermeasurement variation between the two ROIs ranged from 0 to $0.48 \times 10^{-3} \text{ mm}^2 \text{ s}^{-1}$ per measurement. The magnitude of these variations was comparable to reported differences between malignant and non-malignant tissues. These preliminary results, from a small number of subjects, suggest that the menstrual cycle and individual variation in pre-menopausal women should be considered when interpreting the ADC values of uterine structures.

Received 20 March 2008
Revised 20 April 2009
Accepted 11 August 2009

DOI: 10.1259/bjr/11056533

© 2010 The British Institute of
Radiology

Diffusion-weighted imaging (DW) is an emerging functional imaging technique that is based on the diffusion of water molecules [1]. DWI can measure the apparent diffusion coefficient (ADC) of the water in tissue, which reflects its cell density, cellular oedema and microcirculation [1, 2]. Malignant tissue tends to have low ADC values, and so ADCs are increasingly used as a quantitative parameter to distinguish malignant tissue from non-malignant tissue [3–5]. Recent studies in gynaecological imaging have reported ADC values that were lower than normal in uterine cervical cancer, endometrial cancer and leiomyosarcoma [6–8].

In pre-menopausal women, *T*₂ weighted images of the uterus, a three-layer zonal structure, change during the menstrual cycle [9–11]. When the variation in the appearance of the uterus on *T*₂ weighted images and the underlying physiological changes are considered, it seems possible that there might be variation of ADCs in the

normal uterus during the menstrual cycle, which could affect the baseline ADC values used in the assessment of uterine abnormalities. Thus, the purpose of this study was to investigate the ADC values of each zonal structure in the uterus among reproductive women, and their variation in three different phases of the menstrual cycle.

Methods and materials

MR scanning protocol

The study protocol was approved by our institution's ethics committee and written informed consent was obtained from participants. Eleven healthy female volunteers of reproductive age (age range, 24–33 years; mean, 27.8 years), each with a regular menstrual cycle, participated in the study. Exclusion criteria were a history of gynaecological disease, abnormality on MR imaging and the current use of contraceptive medication or methods.

MR scans were scheduled during three phases of the menstrual cycle (menstrual, periovulatory and luteal

Address correspondence to: Masako Kataoka, Department of Radiology, University of Cambridge, Addenbrooke's Hospital, Box 218, Hills Road, Cambridge CB2 0QQ, UK. E-mail: makok@kuhp.kyoto-u.ac.jp; mk435@cam.ac.uk

phases) for each volunteer. The date of ovulation was estimated as either 14 days before the anticipated first day of the next cycle or on the basis of elevated basal body temperature. MR scans were performed in the periovulatory phase within a period two days before or after the expected ovulation date. MR scans in the luteal phase were obtained approximately in the middle of this phase. MR scans in the menstrual phase were obtained within the first 2 days of menstruation.

MR images were obtained with a 1.5 T Symphony scanner (Siemens Medical Systems, Erlangen, Germany) using a phased-array coil. Axial half-Fourier acquisition single-shot turbo spin-echo (HASTE) images, axial and sagittal fast spin-echo T_2 weighted images and sagittal spin-echo T_1 weighted images were obtained to define the anatomy of pelvic organs and to screen for gynaecological abnormalities. No pre-medication agents, including anticholinergic drugs, were administered to participants.

Diffusion-weighted MR imaging in the midsagittal plane of the uterus was performed with a single-shot echo planar imaging (EPI) sequence with the following parameters: repetition time (TR)/echo time (TE), 8000 ms/99 ms; 5 mm slice thickness; field of view (FOV), 260 mm; matrix, 128×46 ; and bandwidth, 1346 (Hz/Pz). The images were acquired using three different b -values ($b = 0, 500$ and 1000 s mm^{-2}) and the chemical shift selective fat suppression (CHESS) technique. The parallel imaging technique was not employed because this technique was not available at the time of this study. ADC maps were automatically created from a series of DW images using a satellite console on the MR unit.

Image analysis

MR images were evaluated by two radiologists. Data analyses were based on final consensus readings. First,

overall quality of ADC maps was evaluated and images with poor image quality (*i.e.* difficult to recognise uterine contours) were excluded from further analysis. Recognition of the (outer) myometrium, endometrium and junctional zone (inner myometrium) on the ADC map was scored on the following three scales: 1= poor, where differentiation of three components was difficult; 2= moderate, where differentiation of three components was possible; 3= excellent, where the three components were clearly differentiated.

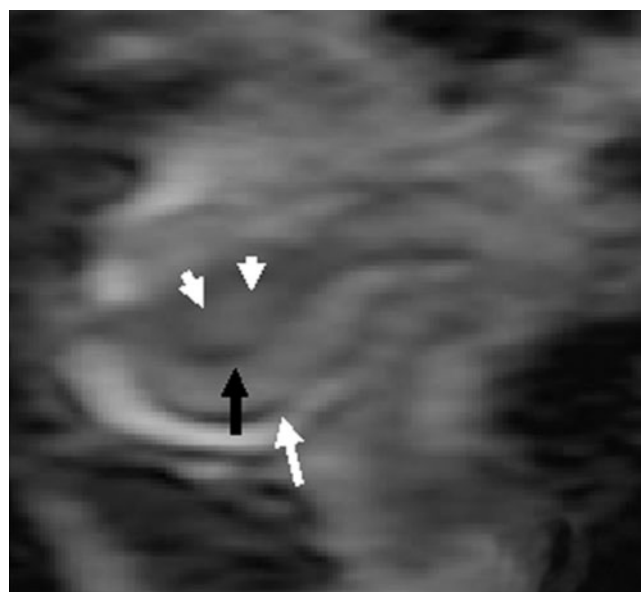
For quantitative analysis, the ADC values of the uterine zonal structures were measured on the ADC map images. Two oval regions of interest (ROI) were placed on the corresponding zonal structures by one radiologist, and the ROI size and ADC values from the two ROIs were measured. We measured two ROIs and used the averaged value, rather than just one ROI, to reduce random variability in the measurements. For the myometrium and junctional zone, one ROI was placed on the anterior wall and another on the posterior wall. The ROIs were selected to be as large as possible, but did not include areas affected by susceptibility artefacts. The mean and standard deviation of the ADC values from seven participants were calculated for each phase. Intra-individual difference, which is the difference between the maximum and minimum ADC values over the three menstrual phases for each participant, was calculated. To determine the general variability of ADC for each woman, the coefficient of variation, which was previously used to report changes in the ADC of breast tissue during menstrual cycles, was calculated using the equation of Partridge et al [12].

As a marker of measurement error, the difference in ADC values between the two ROIs (intermeasurement variation) was also examined.

Figure 1 shows a representative T_2 weighted image and the corresponding ADC map image of the uterus.



(a)



(b)

Figure 1. (a) T_2 weighted image and (b) the corresponding ADC map image of the uterus of a 24-year-old female in the periovulatory phase. Endometrium (white arrowheads), myometrium (white arrow) and junctional zones (black arrows) were clearly recognised in the ADC map image.

Results

Among the 11 participants, two were found to have leiomyomas detectable on MR images and were excluded from the study. Another two participants were excluded from the data analysis because of severe susceptibility artefacts. As a result, seven participants (age range, 24–31 years; mean, 27 years) were evaluated for the recognition of zonal appearance and for quantitative ADC measurement on the ADC map.

With regard to the recognition of uterine zonal anatomy, images from all of the participants were scored as “excellent” in the periovulatory phase, and images from six participants were scored as “excellent” and one as “moderate” in the menstrual and luteal phases. None of the images was scored as “poor”.

The ADCs of each zonal structure were successfully measured in all of the images. The average size of ROI was 0.31 cm² for the myometrium, 0.19 cm² for the endometrium and 0.08 cm² for the junctional zone (inner myometrium). Figure 2 shows the changes in ADC values in the myometrium, endometrium and junctional zone during the different menstrual phases. In the myometrium, the ADC values tended to be lower during the menstrual phase than during the periovulatory and luteal phases, although there was wide variation between individuals. In the endometrium, ADC values again tended to be lower in the menstrual phase than in the other phases, but there was some overlap of values from different individuals. In the junctional zone, ADC values were lowest in the periovulatory phase, followed by the menstrual phase. The maximum–minimum difference in ADC value over the three menstrual phases ranged within the seven individuals from 0.08 to 0.91 ($\times 10^{-3}$ mm²s⁻¹) for myometrium (mean \pm SD, 0.41 ± 0.30 ($\times 10^{-3}$ mm²s⁻¹)); from 0.35 to 0.84 ($\times 10^{-3}$ mm²s⁻¹) (0.55 ± 0.15 ($\times 10^{-3}$ mm²s⁻¹)) for endometrium; and from 0.18 to 0.59 ($\times 10^{-3}$ mm²s⁻¹) (0.40 ± 0.22 ($\times 10^{-3}$ mm²s⁻¹)) for the junctional zone. The coefficient of variation over the different phases was 18% for myometrium, 23% for endometrium and 23% for the junctional zone.

The interindividual maximum–minimum ADC value differences among the seven women for a given zone and phase are shown at the bottom of the graphs in Figure 2. In the myometrium and endometrium, the difference tended to be greatest during the menstrual phase, whereas in the junctional zone this difference tended to be greatest in the periovulatory phase.

Differences (ranges) in measured ADC values between the two ROIs (intermeasurement error) for the periovulatory, luteal and menstrual phases, respectively, were 0.05–0.27 ($\times 10^{-3}$ mm²s⁻¹), 0.02–0.40 and 0.00–0.31 in the myometrium; 0.00–0.31, 0.04–0.15 and 0.00–0.41 for the endometrium; and 0.10–0.48, 0.02–0.34 and 0.02–0.21 for the junctional zone.

Discussion

Our study investigated layer-specific changes in ADC over three different menstrual phases. The ADC values of the myometrium and endometrium tended to be lower in the menstrual phase than in the periovulatory

and luteal phases. The mean intraindividual variation in ADC values over the three menstrual phases was 0.4–0.6 ($\times 10^{-3}$ mm²s⁻¹) on average. The mean Interindividual ADC value variation for a given zone or phase was larger than the intraindividual variation between the phases, and ranged from 0.5 to 0.9 ($\times 10^{-3}$ mm²s⁻¹).

Another study showed a smaller effect of phases of the menstrual cycle on the ADC of breast tissue (coefficient of variation, 5.5%) [12]. This finding differs from ours, possibly because of the different nature of the organs, or the different MRI sequences used. The previous study used single-shot fast spin echo (SSFSE) for DWI, which is less sensitive to susceptibility artefact than EPI, and this might have contributed to the relatively small variation in ADC seen during the menstrual cycle. EPI-based sequences are commonly used in pelvic DWI because of their fast acquisition time and high signal-to-noise ratio [4, 7, 8]. Nevertheless, our results show that baseline changes in the ADC of uterine structures over the different menstrual phases can be large, and hence images should be interpreted carefully.

As ADC value is affected by cell density, cell organisation and microcirculation [1, 2], it is possible that the changes in ADC values seen during the menstrual cycle may reflect phase-specific physiological changes in the structures of the different uterine zones. For the myometrium, oedema in the luteal phase [13] might have contributed to higher ADC values, whereas myometrial contraction and relatively low water content might have reduced ADC values. For the endometrium, the presence of blood in the cavity could be associated with decreased ADC values in the menstrual phase akin to the decreased ADC values seen in acute intracerebral haemorrhage [14] or endometrial cyst [15]. Little is known about physiological or histological changes in the junctional zone, and the observed ADC variation in the junctional zone is therefore difficult to explain.

The magnitude of ADC changes observed over the different menstrual phases, if replicated in larger studies, has implications for the interpretation of ADC values in oncology imaging. The difference between malignant and non-malignant lesions (or normal tissue) in the uterus ranges from 0.45 to 0.65 ($\times 10^{-3}$ mm²s⁻¹) [7, 8], which is comparable to the variation in the ADC of normal structures seen during the three phases of the menstrual cycle in our study. This may be particularly problematic in cases where changes in ADC values are used as a marker of treatment response. Such cases may include treatment of a uterine myometrial or endometrial lesion (e.g. in cervical cancer) in a pre-menopausal patient [6]. Although it is difficult to choose the timing of an MR scan relative to phases of the menstrual cycle in clinical practice, we can consider the menstrual cycle when interpreting ADC values (using either information on menstrual cycle from the patient or the appearance of T₂ weighted images). Most of the uterine lesions lie in either myometrium or endometrium, and these layers showed a similar pattern of ADC value, which tended to drop in the menstrual phase. It would, therefore, be preferable to avoid using ADC measurements obtained during the menstrual phase in order to minimise the effect of menstrual ADC variation on baseline ADC changes.

Relatively large interindividual variation in ADC for any given cycle phase or zone may also affect the interpretation of ADC values in clinical study. Our

Short communication: Changes in ADC in the normal uterus during menstrual phases

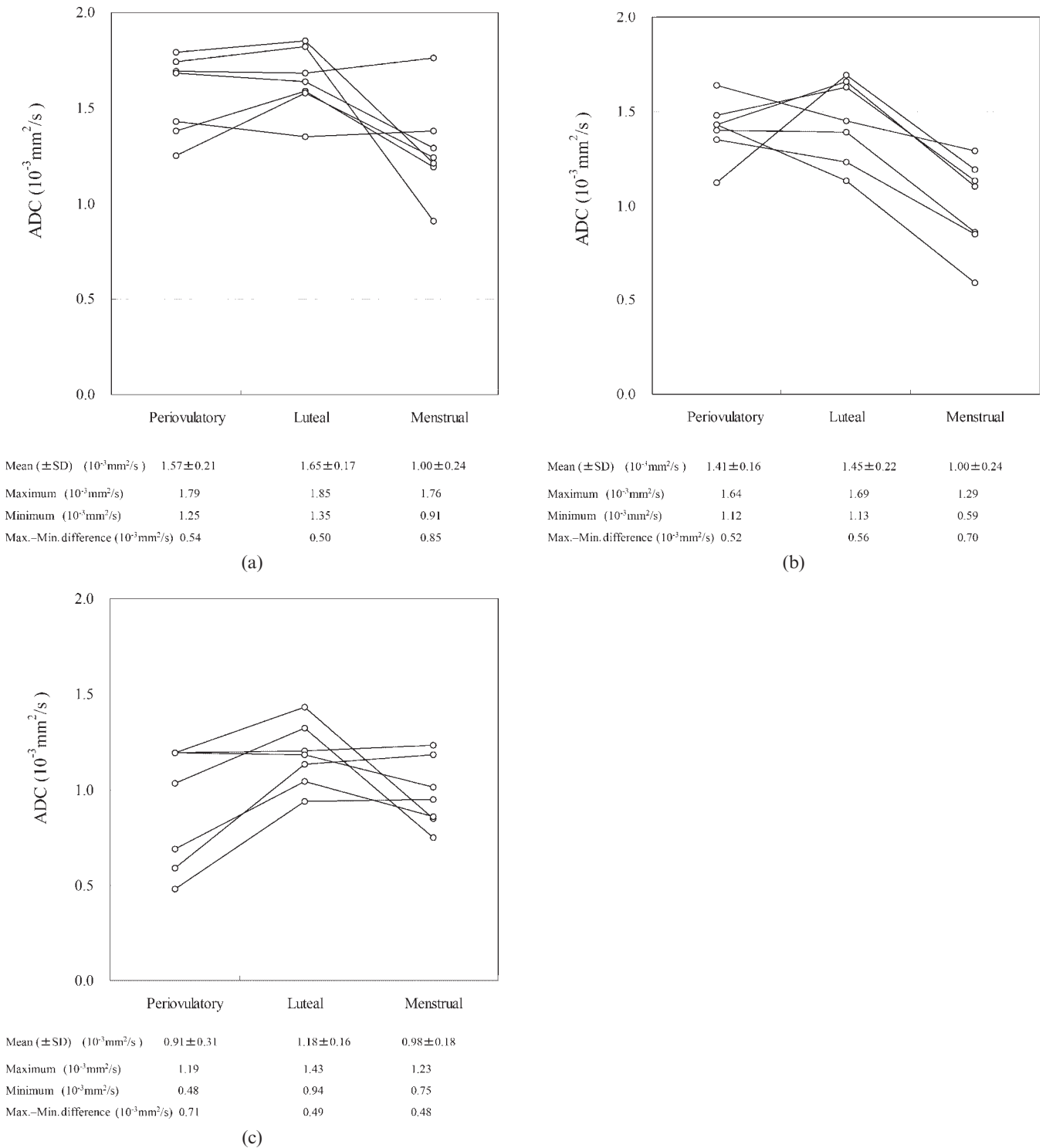


Figure 2. Changes in ADC values ($\times 10^{-3} \text{ mm}^2 \text{ s}^{-1}$) of (a) the myometrium, (b) the endometrium and (c) the junctional zone during three different menstrual phases. Each circle represents the ADC value of a specific tissue layer from a participant in a specific phase. Mean and standard deviation (SD), maximum and minimum ADC values, and the difference between the maximum and minimum ADC values per given phase and zone are shown at the bottom of each graph.

findings suggest that ADC values are more accurate in comparing lesions within a single patient, and that interindividual comparisons require careful interpretation. The interindividual ADC variations in the myometrium and endometrium were greatest in the menstrual phase, at 0.85 and 0.70 ($\times 10^{-3} \text{ mm}^2 \text{ s}^{-1}$), respectively; both of these variations were larger than the reported differences between malignant and non-malignant

lesions. Therefore, ADC value is ideally measured in the perioviulatory or luteal phase.

We used the “menstrual”, “perioviulatory” and “luteal” phases because T_2 weighted MRI images of the uterus showed distinctive changes between these three phases. The uterus of the follicular phase is similar to that of the perioviulatory phase, *i.e.* the junctional zone of the follicular or perioviulatory phases is thinner than that of the menstrual

phase, but thicker than that of the luteal phase. We did not, however, use DWI to examine the uterus in the follicular phase, and this is a possible limitation of this study.

This study has other limitations. First, the results are based on data from a small number of subjects, although both the changes over the three different phases of the menstrual cycle and interindividual variation showed consistent trends. Second, the parallel imaging technique was not available at the time of this study, and this is partially responsible for the severe susceptibility artefact seen in images from two of the participants. Third, ROI analysis is prone to measurement error, the greatest intermeasurement error recorded was as large as $0.45 \times 10^{-3} \text{ mm}^2 \text{ s}^{-1}$. Finally, the menstrual phases of individual participants were not confirmed as accurate by measuring blood hormone levels. Nevertheless, all of the patients had regular menstrual cycles and a large misclassification was unlikely.

In conclusion, we observed changes in ADC values (0.4 to $0.6 (\times 10^{-3} \text{ mm}^2 \text{ s}^{-1})$) in the normal uterus during different menstrual phases. For myometrium and endometrium, the mean ADC value tended to be lower in the menstrual phase than in other phases, although there was some overlap of individual values. The interindividual variation in ADC value for a given zone or phase was even greater than intraindividual variation in ADC value. In addition, intermeasurement variation in ADC value could be as large as $0.5 \times 10^{-3} \text{ mm}^2 \text{ s}^{-1}$. The magnitude of these variations in ADC values is comparable to reported differences between the ADC values of malignant and non-malignant tissues. These preliminary results, from small number of subjects, suggest that the ADC values of uterine structures should be interpreted in the light of the phase of the menstrual cycle and interindividual differences in pre-menopausal women.

Acknowledgments

The authors thank Akira Hiraga and Ari Kobayashi (Kyoto University Hospital) for their technical assistance.

References

1. Le Bihan D, Turner R, MacFall JR. Effects of intravoxel incoherent motions (IVIM) in steady-state free precession (SSFP) imaging: application to molecular diffusion imaging. *Magn Reson Med* 1989;10:324–37.
2. Lyng H, Haraldseth O, Rofstad EK. Measurement of cell density and necrotic fraction in human melanoma xenografts by diffusion weighted magnetic resonance imaging. *Magn Reson Med* 2000;43:828–36.
3. Koh DM, Padhani AR. Diffusion-weighted MRI: a new functional clinical technique for tumour imaging. *Br J Radiol* 2006;79:633–5.
4. DeSouza NM, Reinsberg SA, Scurr ED, Brewster JM, Payne GS. Magnetic resonance imaging in prostate cancer: the value of apparent diffusion coefficients for identifying malignant nodules. *Br J Radiol* 2007;80:90–5.
5. Vandecaveye V, de Keyzer F, Vander Poorten V, Deraedt K, Alaerts H, Landuyt W, et al. Evaluation of the larynx for tumour recurrence by diffusion-weighted MRI after radiotherapy: initial experience in four cases. *Br J Radiol* 2006;79:681–7.
6. Naganawa S, Sato C, Kumada H, Ishigaki T, Miura S, Takizawa O. Apparent diffusion coefficient in cervical cancer of the uterus: comparison with the normal uterine cervix. *Eur Radiol* 2005;15:71–8.
7. Tamai K, Koyama T, Saga T, Umeoka S, Mikami Y, Fujii S, et al. Diffusion-weighted MR imaging of uterine endometrial cancer. *J Magn Reson Imaging* 2007;26:682–7.
8. Tamai K, Koyama T, Saga T, Morisawa N, Fujimoto K, Mikami Y, et al. The utility of diffusion-weighted MR imaging for differentiating uterine sarcomas from benign leiomyomas. *Eur Radiol* 2008;18:723–30.
9. Haynor DR, Mack LA, Soules MR, Shuman WP, Montana MA, Moss AA. Changing appearance of the normal uterus during the menstrual cycle: MR studies. *Radiology* 1986;161:459–62.
10. Demas BE, Hricak H, Jaffe RB. Uterine MR imaging: effects of hormonal stimulation. *Radiology* 1986;159:123–6.
11. McCarthy S, Tauber C, Gore J. Female pelvic anatomy: MR assessment of variations during the menstrual cycle and with use of oral contraceptives. *Radiology* 1986;160:119–23.
12. Partridge SC, McKinnon GC, Henry RG, Hylton NM. Menstrual cycle variation of apparent diffusion coefficients measured in the normal breast using MRI. *J Magn Reson Imaging* 2001;14:433–8.
13. Silverberg SG, Kurman RJ. Tumor of the uterine corpus and gestational trophoblastic disease. In: Rosai J, editor. *Atlas of Tumor Pathology*. Washington, D.C.: Armed Forces Institute of Pathology, 1992: 1–8.
14. Kang BK, Na DG, Ryoo JW, Byun HS, Roh HG, Pyeun YS. Diffusion-weighted MR imaging of intracerebral hemorrhage. *Korean J Radiol* 2001;2:183–91.
15. Moteki T, Ishizaka H. Diffusion-weighted EPI of cystic ovarian lesions: evaluation of cystic contents using apparent diffusion coefficients. *J Magn Reson Imaging* 2000;12:1014–19.